*Int. J. Electrochem. Sci.*, 14 **(2019)** 10862 – 10869, doi: 10.20964/2019.12.09

International Journal of
ELECTROCHEMICAL
SCIENCE
www.electrochemsci.org

*Short Communication*

# Photocatalytic Activities of Vertically Aligned Manganese-Doped ZnO Nanorods Synthesized on ITO Film by Electrochemical Technique

*Liqun Fan, Jinhu Wang, Na Qiu, Yong Liu*, Xianman Zhang*

College of Chemistry, Chemical Engineering and Materials Science, Zaozhuang University, Zaozhuang, shandong 277160, China
*E-mail: liuyong20049@163.com

*Received:* 6 June 2019 / *Accepted:* 5 August 2019 / *Published:* 29 October 2019

A facile electrochemical approach was used to one step growth of Mn-doped ZnO nanorods on indium tin oxide conductive glass. FESEM images show an increase in diameter and height of ZnO nanorods by doping Mn ions in ZnO lattice. XRD results indicate that the Mn dopant lead to a shift in the diffraction peak position toward a lower angle side compared to the undoped ZnO nanorods. Electrochemical impedance spectroscopy results proving that doping Mn ions in ZnO nanorods can lead to higher free-electron carriers that accelerate charge transfer and reduces the resistance. Photocatalytic activities of the sample were studied by degrading methylene blue under UV–vis light irradiation. The photodegradation efficiency of Mn-doped ZnO nanorods achieved for 100 min irradiation times was 81% which reveals better findings compared to previous reports. The Mn-doped ZnO nanostructures have higher rate constant and degradation efficiency as it has higher surface defects, length, and crystallinity than others.

**Keywords:** Mn-doped ZnO nanorods; Photocatalytic activities; Electrochemical impedance spectroscopy; Electrochemical technique

## 1. INTRODUCTION

Photocatalysis has been entrenched as a productive process used in mineralization of toxic organic compounds, hazardous inorganic constituents and bacteria disinfection after Fujishima and Honda decomposed water into hydrogen and oxygen using a titanium electrode in 1972, due to its strong oxidizing hydroxyl agent [1]. Some active metal oxide semiconductors that are proven to be photocatalysts are TiO2, ZnO, WO3, and Fe2O3 [2-6].

Highly active electrons and holes are generated by these semiconductors that have the ability to perform pollutant degradation in water with light. Photocatalytic oxidation has been the center of

attention due to its excellent features like cost-effectiveness, low-toxicity, energy-efficient, reusability, and no secondary pollution [7].

The highly transparent visible domain along with high UV radiation absorbency due to its special optical properties contributes to the investigation of ZnO as a coating material, from paints to sunscreens and fabric coating. The photocatalytic activity of ZnO is widely accepted and has been applied in various concepts to investigate [8, 9]. The high photocatalytic activity of ZnO is favorable for some applications, but for applications like fabric or paper coating, it is unfavorable as ZnO capacity for degradation of the organic substrate is a hindrance [10].

Even though, the attention gained by UV-photo induced reactions on the transition metal-doped ZnO in the slurry is high, very little study has been done on the effect of dopants [11]. Some researchers have reported that doping of ZnO with Mn increases the photocatalytic activity up to 2 mol% under UV irradiation while some others have reported the opposite results [12]. Barick et al. synthesized pure and doped ZnO nanoclusters and compared their photocatalytic activity of MB dye degradation under UV light [13]. They found pure ZnO to be a better photocatalyst as compared to transition metal doped ZnO. Dodd et al. investigated the effect of cobalt and manganese oxide on the photocatalytic activity of ZnO nanoparticles [12]. The enhanced photocatalytic activity was observed for a dopant level of 2 mol% in the case of Mn doping. Thereafter an increase in dopant concentration to 5 mol% resulted in a drop of photocatalytic activity of ZnO. Tsuzuki et al. evaluated the photocatalytic activity of undoped and Mn-doped ZnO nanoparticles for the degradation of RhB dye and observed that doping with Mn reduced the photocatalytic activity of ZnO [14].

To the best of our knowledge, for the first time in this research, the one step electrochemical method was used to synthesize Mn-doped ZnO nanorods and their photocatalytic decolorization activities using methylene blue (MB) as a model have been reported.

## 2. MATERIALS AND METHOD

Indium tin oxide(ITO) substrates were deposited with 100 nm thick ZnO layer with a magnetron sputter, before the electrochemical deposition experiment. ZnO nanostructures were grown by two electrode electrochemical Teflon cell and the aqueous solution inside the cell was heated by a hot plate heater. 25 mM of zinc nitrate hydrate ($Zn(NO_3)_2 6H_2O$, 99.99%) and 25 mM of hexamethylenetetramine (HMT; $C_6H_{12}N_4$, 99%) were dissolved in deionized water (50 ml) under magnetic stirring to form the solution for nanorods growth. For the experimental synthesis of Mn-doped ZnO, 1 M HMT, 1 M Zinc acetate dihydrate and manganese tetrachloride with concentration 5 mol% were dissolved individually in 25 ml DI water respectively. Ammonia was added to the solution for pH adjustment to 10 and is mixed for 3h. This solution was poured into the galvanic cell. The Pt electrode as anode and coated ZnO seed layer on ITO as a cathode is placed inside the galvanic cell. ZnO nanorods grown in vertical alignment was produced with 0.3 $mA/cm^2$ current density, 95 C temperature, and 1-hour growth time. The samples were washed using DI water and dried by N2 gas.

Field emission scanning electron microscopy (FE-SEM, FEI Sirion 200) and XRD (PANalytical, X'Pert PRO) measurement were done to investigate the morphology and crystal quality of the

synthesized ZnO nanostructure. An energy-dispersive X-ray (EDX) spectrometry was used to examine the detailed elemental analysis of the samples. UV-vis spectrophotometer (UV-1800, Shimadzu, Kyoto, Japan) was used to record the UV-vis spectra of the gelatin/ZnO NR bio-nanocomposite films. Electrochemical impedance spectroscopy (EIS) was used to examine the charge transfer and recombination processes with a potential of 10 mV at frequencies range from 0.1 Hz to 0.1MHz. High-performance methylene blue (MB) dye was used to inspect the qualitative identification of the undoped and Mn-doped ZnO nanorods and photocatalytic degradation of undoped and Mn-doped ZnO specimens.

## 3. RESULTS AND DISCUSSION

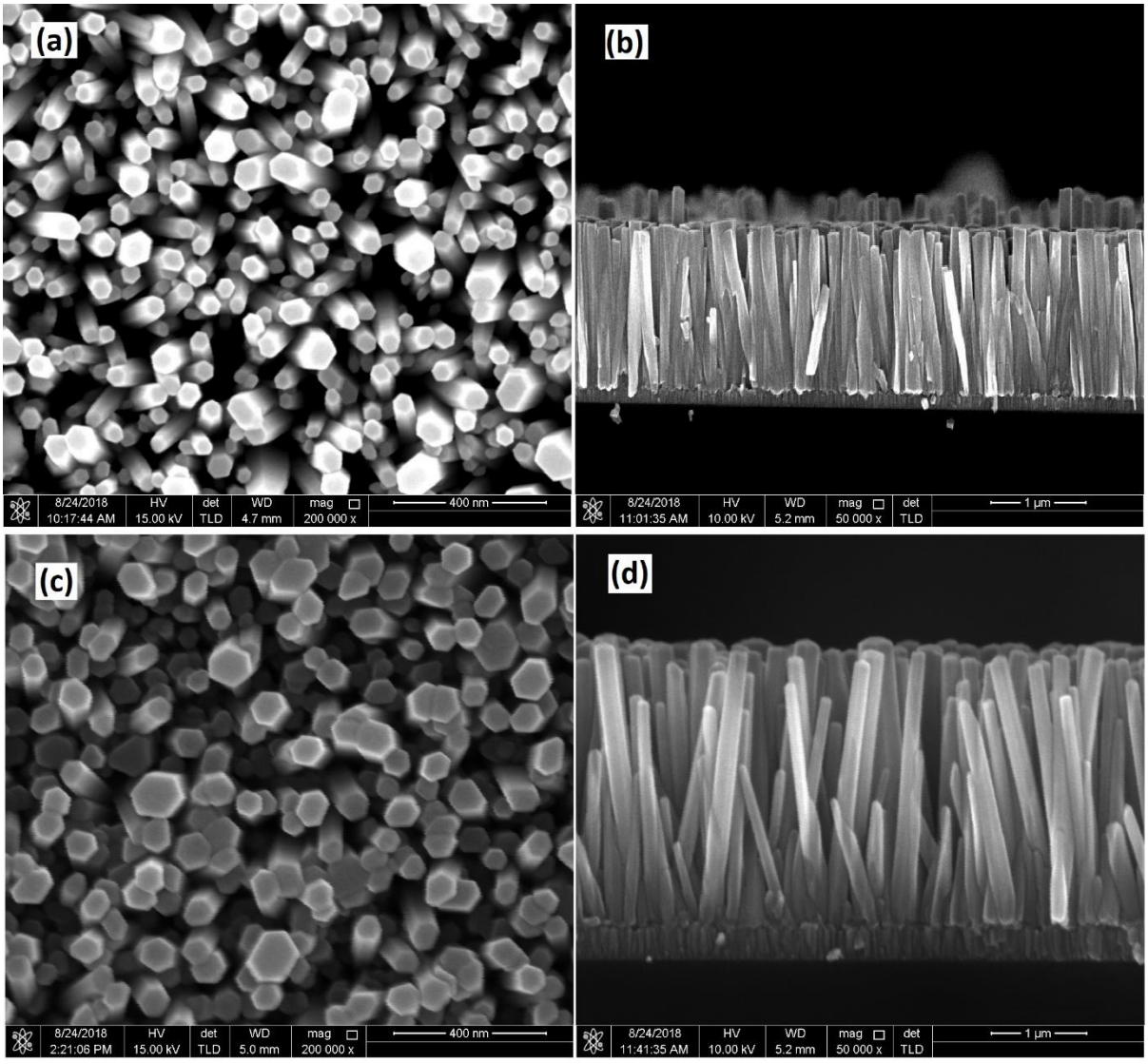


**Figure 1.** FESEM images (a) Top and (b) Cross section of undoped and (c) Top and (d) Cross section of Mn-doped ZnO nanorods

The surface morphology of ZnO nanorods can be seen from the FESEM images in Fig. 1. The growth of ZnO as hexagonal nanorods in the direction perpendicular to the glass substrate surface can be found in samples. After doping with Mn ions, the diameters of the undoped ZnO nanorods increased. The diameters of the undoped and Mn-doped ZnO were in the range of 100-180 nm and 110-250 nm, respectively. The quantity of nanorods also increases when the dopant is added. The number of undoped and 5 mol% Mn-doped ZnO nanostructures are about 13 $\mu m^{-2}$ and 21 $\mu m^{-2}$, respectively.

The measured surface area for the undoped ZnO is about 10 $\mu m^2$ substrate while for doped ZnO, it is about 26 $\mu m^2$ substrate. As shown in the nanorod cross-sectional images, doping with Mn ions increases the average length of the ZnO nanorods. 1.74 and 2.27 μm were the average length of the undoped and doped nanorods, respectively. Fig 1 shows images with nanorods proving that the diameter increase with a dopant amount. Reports have been made earlier on how doping influences the ZnO morphology [3]. The reports by Panigrahy et al. stated that the diameter of ZnO nanorods increased from 85 to 150 nm with 5 mol% Mn dopant and from 120–400 nm to 120–700 nm with 2 mol% Mn [15, 16]. As seen from the evidence such as increment in diameter, length, and a quantity of nanorods in a surface area, it is clear that the enhancement of the ZnO crystal growth is influenced by the Mn elements.

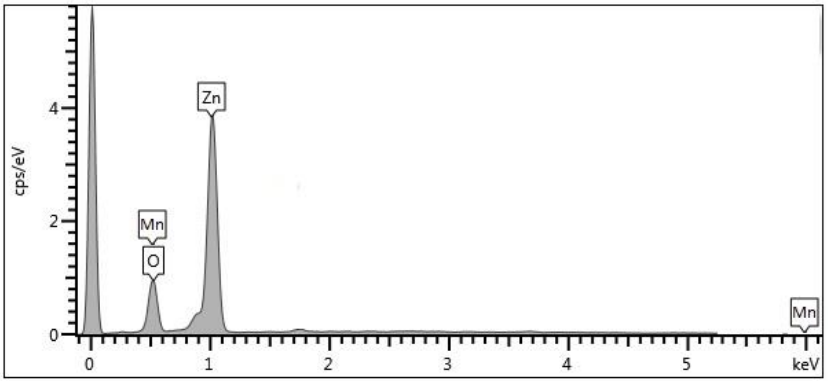


**Figure 2.** EDAX spectra of Mn-doped ZnO nanostructures

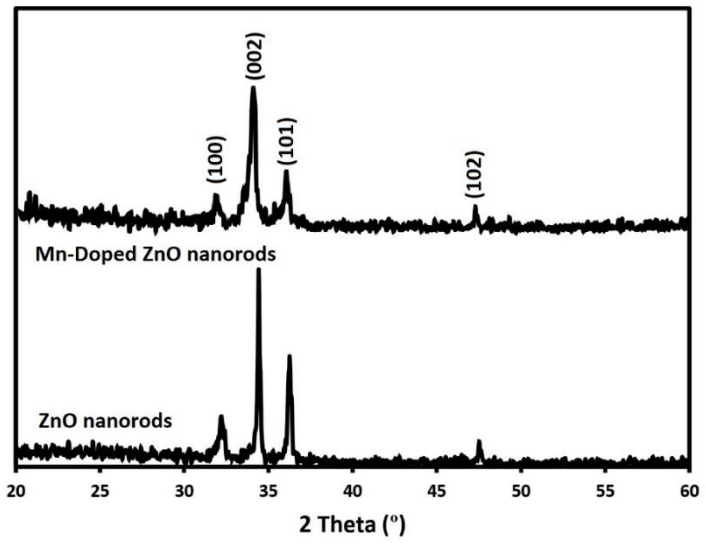


**Figure 3.** The XRD pattern of the undoped and Mn-doped ZnO nanorods

EDAX spectra of Mn-doped ZnO nanostructures in Fig. 2 detects the existence of elements in the sample. The spectra of 5% Mn-doped ZnO showed peaks with atomic concentrations such as Mn – 3.41%, Zn – 30.23%, and ZnO – 66.36%. Mn substitution in ZnO lattice was found.

The XRD pattern of the Mn-doped ZnO nanorods is shown in figure 3. The pattern showed only peaks that can be indexed to hexagonal wurtzite ZnO structure (JCPDS No. 36 - 1451), without secondary peaks from possible impurities like Mn oxides. The Mn dopant addition favors a shift in the diffraction peak position at a lower angle side compared to the pure ZnO nanorods. The shift may be due to a decrease in doped Mn concentration along with the diffused sample depth and from the surface to the core of a single ZnO nanorod. It is in relation to the $Zn^{2+}$ substituted with $Zn^{2+}$ as the ionic radius is smaller than $Mn^{2+}$ (0.083 nm). The substitution of $Zn^{2+}$ by $Mn^{2+}$ is accurately evidenced by the peak shift in the lower angles.

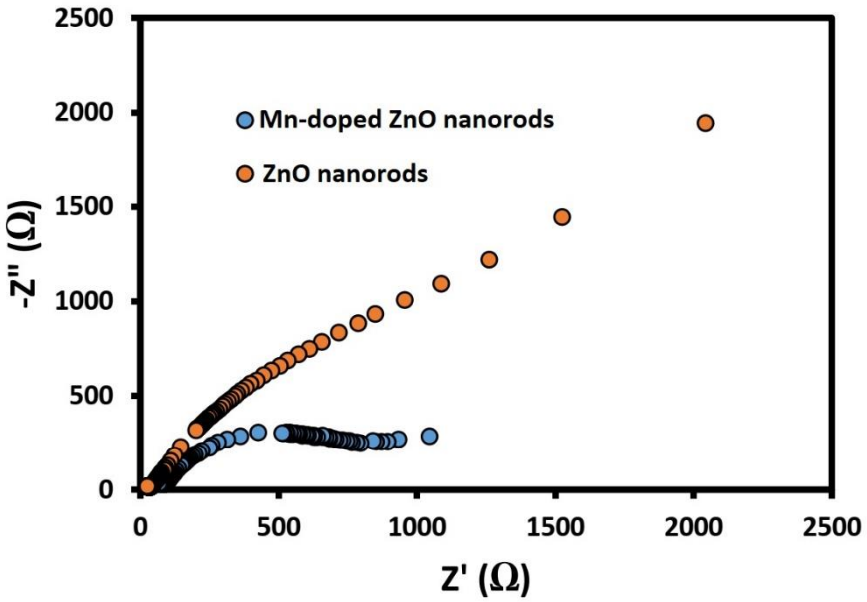


**Figure 4.** Nyquist plots of undoped and Mn-doped ZnO nanorods

In order to complete the information about the charge transfer efficiency and interface charge separation of ZnO photocatalysts [17], the electrochemical impedance measurement was done. Fig. 4 indicates a Nyquist plot between an imaginary and real impedance for ZnO nanorods with Mn doping. The radius of the arc reflects the resistance of interface layer at the surface of electrode. As the efficiency of the charge transfer decreases, the arc radius increases. An increase in Mn doping decreases the interface layer resistances, showing the developed efficiency of charge transfer and interfacial charge-carrier separation on the surface of ZnO. These results are proving that doping Mn ions in ZnO nanorods can lead to higher free-electron carriers that accelerate charge transfer and reduces the resistance, it is useful for the photocatalytic activity enhancement of ZnO nanorods.

One of the most difficult natural dye to degrade is Methylene blue (MB). Photocatalytic activities of the sample were studied by degrading methylene blue. It was evaluated under UV–vis light irradiation using 10 mm×10 mm thin films of undoped and Mn-doped ZnO.

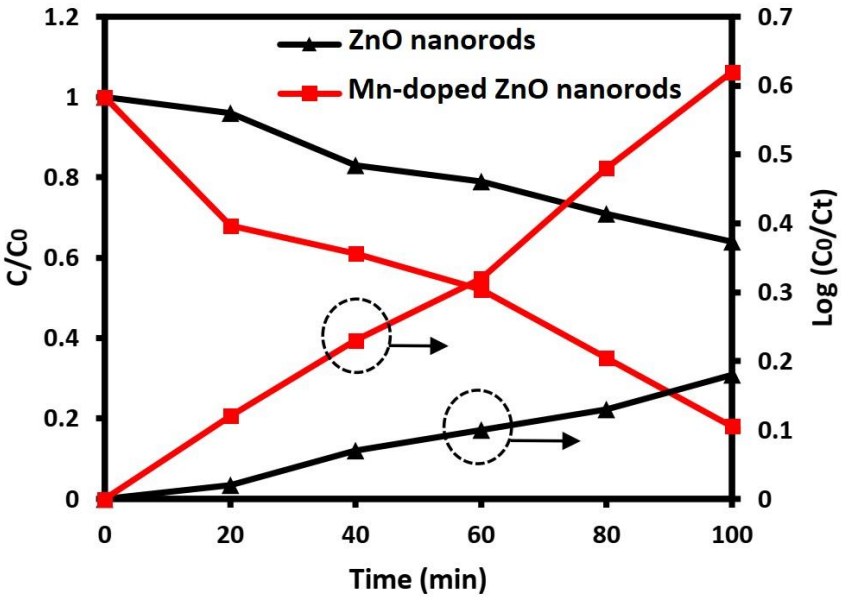


**Figure 5.** Plots of (a) $C/C_0$ (b) log $C_0/C_t$ versus irradiation time for the undoped and Mn-doped ZnO nanorods

The photodegradation percentage plot at various irradiation time is shown in Figure 5. The photodegradation efficiency is introduced as the highest photodegradation at one hour was determined by the following relationship:

$$Photodegradation\ efficiency\ (\%)\left(\frac{C_0-C_{100}}{C_0}\right)\times 100 \qquad (1)$$

Table 1 depicts the Pseudo-first-order (PFO) rate constant and photodegradation efficiency of undoped and Mn doping ZnO nanorods. It was confirmed that the Mn-doped ZnO nanostructures have better photodegradation efficiency because of the effective charge carrier transport to the length of ZnO nanorods. Kinetic studies were performed for undoped and Mn-doped ZnO specimens which are revealed in Figure 5.

**Table 1.** Results of photodegradation efficiency and PFO rate constant of undoped and Mn-doped ZnO nanorods

| **Samples** | **Photodegradation efficiency (%)** | **Pseudo-first-order rate constant (k)** |
|---|---|---|
| Undoped ZnO nanorods | 38 | 0.0942 |
| Mn-doped ZnO nanorods | 82 | 0.3114 |

Our samples follow PFO kinetics relation for photodegradation of MB which is shown in following relation [18]:

$$log\frac{C_0}{C_t} = kt \quad (2)$$

where, k is the PFO rate constant that was determined using the plot slope of $logC_0/C_t$ versus time of irradiation. A higher rate constant was detected in Mn-doped ZnO. More active sites were seen in nanowires with large surface area that absorbed organic compounds for photodegradation. The Mn-doped ZnO nanostructures have higher rate constant and degradation efficiency as it has higher surface defects, length, and crystallinity than others. Ma et al. described that it requires 4 h for degradation of MB to reach 90% [19]. The rate constant in this study was better than previous reports, where the degradation efficiency achieved for one hour was 81%.

**Table 2.** Overview of the different transition metals-doped ZnO nanostructures with their synthesis techniques and photocatalytic performances.

| Doping materials | Synthesis technique | Pollutant | Time (min) | Deg. (%) | Ref. |
|---|---|---|---|---|---|
| **Cu** | Thermal decomposition process | Methylene blue | 60 | 77.3 | [20] |
| **Ag** | Sol–gel method | Methylene blue | 120 | 95 | [21] |
| **Au** | Surfactant free phytochemical reduction | Methylene blue | 180 | 76 | [22] |
| **Mn** | Ion-exchange method | Methylene blue | 240 | 90 | [19] |
| **Mn** | Electrochemical method | Methylene blue | 60 | 81 | This work |

Table 2 shows Ag, Cu, Au and Mn transition metals effect on the photodegradation of MB dye. In comparison with previous reported works containing transition elements doped ZnO photocatalysts, Mn-doped ZnO photocatalyst has the highest photocatalytic activity under UV light. It can be attributed to lower recombination between photogenerated electrons and holes and hence needs a high degree of crystallinity than a high surface area. The findings indicate that Mn doping materials can be an alternative dopant for developing photocatalytic treatment.

## 4. CONCLUSION

We report the photocatalytic activities of undoped and Mn-doped ZnO nanorods. Mn-doped ZnO specimens were synthesized using an electrochemical method. FESEM, EDX and XRD techniques were utilized to characterize the synthesized samples. FESEM images show an increase in diameter and height of ZnO nanorods by doping Mn ions in ZnO lattice. The XRD analysis confirms the presence of wurtzite phase of all the samples. The photodegradation activities of undoped and Mn-doped ZnO photocatalysts were assessed using a basic MB as organic pollutant with UV light irradiation. The experimental results reveal that the photodegradation efficiency of doping $Mn^{2+}$ ions in ZnO lattice is significantly higher

than that of undoped ZnO in comparison with previous reports. It can be attributed to higher free-electron carriers that accelerate charge transfer and reduces the resistance which is useful for the photocatalytic activity enhancement of ZnO nanorods.

ACKNOWLEDGEMENTS
The study was supported by Natural Science Foundation of Shandong Province with Grant No. ZR201702200464 and ZR2019QB013.

**References**

1. B. Viswanathan, *Natural Resources & Engineering*, 2 (2017) 1.
2. K. Qi, B. Cheng, J. Yu and W. Ho, *Chinese Journal of Catalysis*, 38 (2017) 1936.
3. M. Samadi, M. Zirak, A. Naseri, E. Khorashadizade and A.Z. Moshfegh, *Thin Solid Films*, 605 (2016) 2.
4. A. Hammad, H.M. El-Bery, A. EL-Shazly and M. Elkady, *International Journal of Electrochemical Science*, 13 (2018) 362.
5. J. Rouhi, C.R. Ooi, S. Mahmud and M.R. Mahmood, *Materials Letters*, 147 (2015) 34.
6. N. Naderi, M. Hashim, K. Saron and J. Rouhi, *Semiconductor Science and Technology*, 28 (2013) 025011.
7. X. Lian and B. Yan, *Inorganic chemistry*, 55 (2016) 11831.
8. W. Yu, J. Zhang and T. Peng, *Applied Catalysis B: Environmental*, 181 (2016) 220.
9. E. Rokhsat and O. Akhavan, *Applied Surface Science*, 371 (2016) 590.
10. F. Zhang, W. Zhang, X. Luo, G. Feng and L. Zhao, *International Journal of Electrochemical Science*, 12 (2017) 3756.
11. S. Ekambaram, Y. Iikubo and A. Kudo, *Journal of alloys and compounds*, 433 (2007) 237.
12. A. Dodd, A. McKinley, T. Tsuzuki and M. Saunders, *Materials chemistry and physics*, 114 (2009) 382.
13. K. Barick, S. Singh, M. Aslam and D. Bahadur, *Microporous and Mesoporous Materials*, 134 (2010) 195.
14. T. Tsuzuki, R. He, J. Wang, L. Sun, X. Wang and R. Hocking, *International journal of nanotechnology*, 9 (2012) 1017.
15. B. Sambandam, R.J.V. Michael and P.T. Manoharan, *Nanoscale*, 7 (2015) 13935.
16. R. Ullah and J. Dutta, *Journal of Hazardous materials*, 156 (2008) 194.
17. M. Husairi, J. Rouhi, K. Alvin, Z. Atikah, M. Rusop and S. Abdullah, *Semiconductor Science and Technology*, 29 (2014) 075015.
18. B.P. Nenavathu, S. Kandula and S. Verma, *RSC Advances*, 8 (2018) 19659.
19. Q. Ma, X. Lv, Y. Wang and J. Chen, *Optical Materials*, 60 (2016) 86.
20. T. Bhuyan, M. Khanuja, R. Sharma, S. Patel, M. Reddy, S. Anand and A. Varma, *Journal of Nanoparticle Research*, 17 (2015) 288.
21. P. Amornpitoksuk, S. Suwanboon, S. Sangkanu, A. Sukhoom, N. Muensit and J. Baltrusaitis, *Powder Technology*, 219 (2012) 158.
22. M.K. Choudhary, J. Kataria and S. Sharma, *ACS Applied Nano Materials*, 1 (2018) 1870.